ZAG Regulates the Skin Barrier and Immunity in Atopic Dermatitis

Ji Yeon Noh[1,5], Jung U Shin[1,4,5], Ji Hye Kim[1], Seo Hyeong Kim[1], Bo-Mi Kim[1], Young Hwan Kim[2], Semin Park[2], Tae-Gyun Kim[1], Kyong-Oh Shin[3], Kyungho Park[3] and Kwang Hoon Lee[1]

Adipokines modulate immune responses and lipid metabolism in allergic disease; however, little is known about their role in the skin barrier and atopic dermatitis (AD). We identified ZAG, an adipokine that regulates lipid mobilization, as a biomarker for AD. ZAG levels were consistently decreased in sera, T cells, and skin in human AD patients compared with healthy controls. ZAG was primarily detected in the stratum corneum along with FLG and LOR. Knockdown of ZAG with short hairpin RNA resulted in decreased FLG and increased TSLP. Topical ZAG treatment in AD mice recovered ZAG expression in the skin and improved AD-like symptoms, transepidermal water loss, and ceramide levels. Furthermore, topical ZAG treatment induced immunoregulatory effects, including reduction of IL-4, IL-17, and IFN-γ and increased Foxp3 in the skin and lymphoid organs. Interestingly, ZAG treatment also recovered decreased levels of ADAM17, an important player in skin barrier function and immune response in AD. Thus, ZAG deficiency is closely related to skin barrier function and the immune abnormalities of AD, and we suggest that restoration of ZAG may be a promising therapeutic option for the treatment of AD.

Journal of Investigative Dermatology (2019) **139,** 1648–1657; doi:10.1016/j.jid.2019.01.023

INTRODUCTION

Atopic dermatitis (AD) is a chronically relapsing inflammatory skin disease caused by complex interplay between the immune system and skin barrier abnormalities (Bieber, 2008; Boguniewicz and Leung, 2011). Patients with AD commonly demonstrate allergic immune characteristics, such as increased serum IgE levels, T helper type 2 cytokine secretion (IL-4, IL-5, and IL-13), and increased expression of FcεRI on lesional dendritic cells (Malik et al., 2017). Skin barrier abnormalities in patients with AD are typically associated with altered extracellular lipid composition in the stratum corneum and with FLG gene mutations (Palmer et al., 2006).

Adipokines have been reported to modulate immune responses and lipid metabolism in allergic disease (Tilg and Moschen, 2006). A previous report showed that serum levels of leptin were increased in allergic asthma patients (Guler et al., 2004), and forced expression of leptin in a murine allergen-induced asthma model exacerbated asthmatic inflammation, suggesting a pro-inflammatory role for leptin in allergic inflammation (Shore et al., 2005). Furthermore, leptin induces pro-inflammatory activity by $CD4^+$ T cells, increasing T-lymphocyte proliferation, and production of cytokines, especially IL-1, IL-12, and TNF-α (Saucillo et al., 2014). In contrast, adiponectin exerts anti-inflammatory effects in allergy pathogenesis (Shore et al., 2006), inhibiting lipogenesis and expression of inflammatory genes, such as IL-6, via modulation of NF-κB and activation of extracellular signal–regulated kinase (Tang et al., 2007).

Although several studies have provided insight into the role of adipokines in allergy pathogenesis, relatively little is known about the function of adipokines in AD (Balato et al., 2011; Han et al., 2016; Machura et al., 2013; Nagel et al., 2009). In this study, we discovered that the adipokine ZAG is a candidate biomarker and therapeutic target for AD.

ZAG is a 41-kDa protein that is detected in various body fluids and produced by adipocytes and keratinocytes in the skin (Bao et al., 2005; Chen et al., 2000; Hale, 2002). ZAG functions in lipolysis in adipocytes via the β-adrenergic receptor (Russell and Tisdale, 2012). ZAG contains a large groove that is analogous to the class I major histocompatibility complex peptide-binding groove and two fatty acid-binding sites (Sanchez et al., 1999), indicating a possible role for this protein in immunomodulation (Zahid et al., 2016). Additionally, ZAG has been shown to be associated with terminal differentiation of epidermal keratinocytes (Chen et al., 2000) and fatty acid metabolism (Bing et al., 2010; Hassan et al., 2008). Here, we report a role for ZAG in AD pathogenesis and demonstrate that topical ZAG treatment restores skin barrier integrity and AD inflammation, possibly via effects on ADAM17.

RESULTS

ZAG expression is consistently reduced in both sera and skin of AD patients

To identify targets in AD pathogenesis, we performed 2-dimensional difference gel electrophoresis analysis of sera

[1]*Department of Dermatology and Cutaneous Biology Research Institute, Yonsei University College of Medicine, Seoul, Korea;* [2]*Biomedical Omics Group, Korea Basic Science Institute, Cheongju, Korea;* [3]*Department of Food Science and Nutrition, and Convergence Program of Material Science for Medicine and Pharmaceutics, Hallym University, Chuncheon, Korea; and* [4]*Department of Dermatology, CHA Bundang Medical Center, CHA University, Seongnam, Korea*

[5]*These authors contributed equally to this work.*

Correspondence: Kwang Hoon Lee, Department of Dermatology and Cutaneous Biology Research Institute, Yonsei University College of Medicine, 50 Yonsei-ro, Seodaemungu, Seoul, Korea. E-mail: kwanglee@yuhs.ac

Abbreviations: AD, atopic dermatitis; CER, ceramide; HC, healthy control; qRT-PCR, quantitative real-time polymerase chain reaction; shRNA, short hairpin RNA; NHEK, normal human epidermal keratinocyte

Received 3 August 2018; revised 10 January 2019; accepted 24 January 2019; accepted manuscript published online 6 February 2019; corrected proof published online 25 April 2019

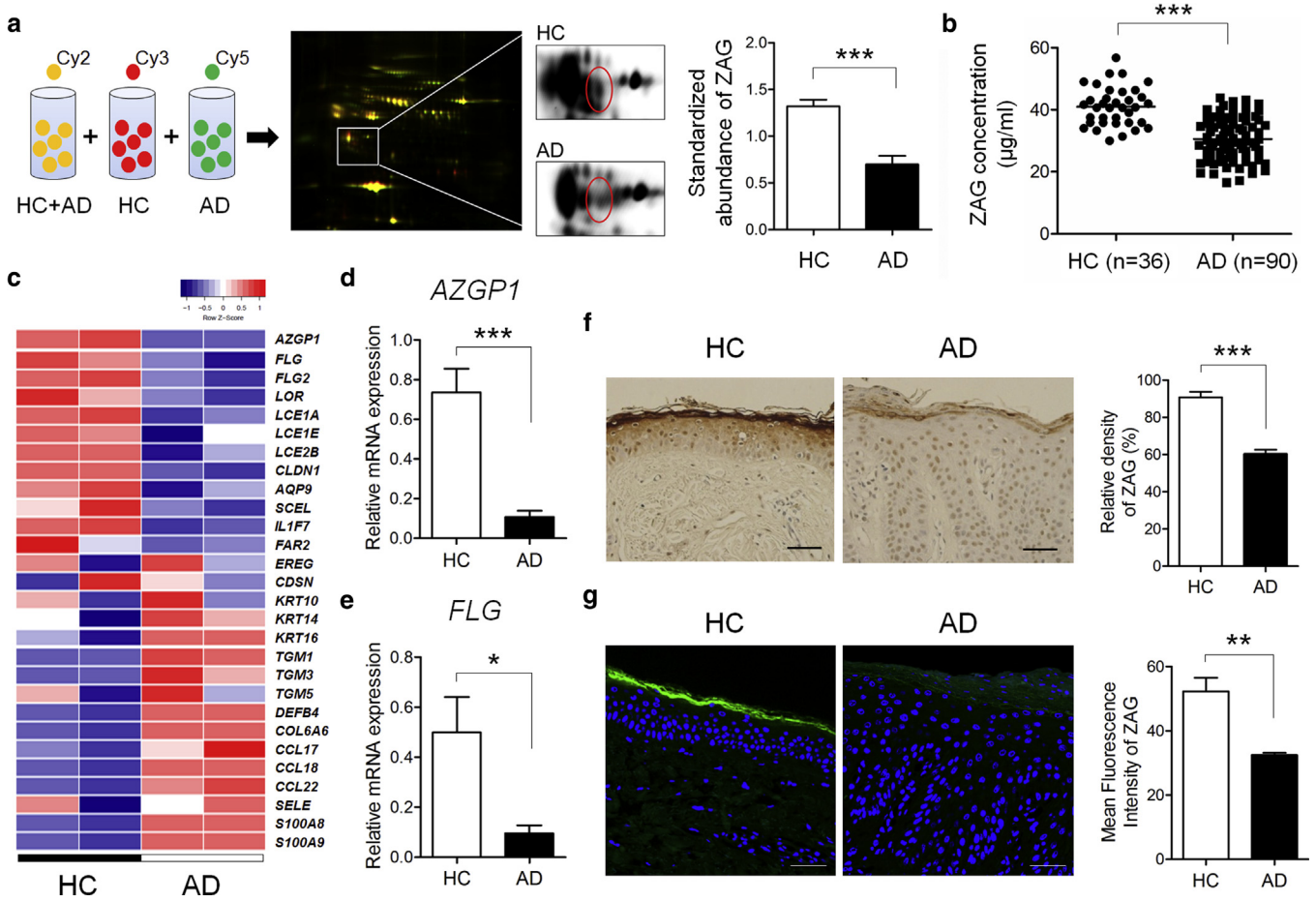

Figure 1. Decreased ZAG expression in both sera and skin of human HC and AD patients. (**a**) 2-Dimensional difference gel electrophoresis analysis was performed to evaluate differential expression of proteins between HC and AD sera (***$P < 0.001$). (**b**) ZAG was measured in sera of HC and AD patients using ELISA (***$P < 0.001$). (**c**) Heatmap of RNA expression levels of ZAG and skin barrier genes in HC and AD skin. Quantitative real-time PCR analyses show (**d**) *AZGP1* and (**e**) *FLG* expression in HC and AD skin. Expression of ZAG in HC and AD skin and its localization is demonstrated by (**f**) immunohistochemical and (**g**) immunofluorescence staining (**$P < 0.01$, ***$P < 0.001$). Scale bar = 50 μm. Quantitated data are presented as mean ± standard error of the mean. AD, atopic dermatitis; HC, healthy control.

from AD patients and healthy controls (HC). We identified one of the most significantly altered proteins as ZAG using tandem mass spectrometry analysis (Figure 1a) and confirmed expression of ZAG by ELISA (Figure 1b). ZAG was decreased in sera from AD patients compared to HC (***$P < 0.001$, Figure 1b). However, there was no correlation between ZAG and the Eczema Area and Severity Index in either serum or skin samples (data not shown). We next performed microarray analysis and found decreased mRNA expression of the ZAG coding gene, *AZGP1*, in AD skin compared to HC (Figure 1c) and also confirmed by quantitative real-time polymerase chain reaction (qRT-PCR; Figure 1d). We also demonstrated that *FLG* expression is decreased in the skin of AD patients using microarray and qRT-PCR analysis (Figure 1c, 1e), as reported previously (Suarez-Farinas et al., 2011). In accordance with the reduction of ZAG and FLG, expression of other skin barrier proteins, such as *LOR*, *CLDN1*, *AQP9*, and *TGM1*, were altered in AD skin (Figure 1c). Furthermore, immunohistochemistry and immunofluorescence staining showed that ZAG was significantly reduced in the stratum corneum of AD skin (Figure 1f, 1g). Collectively, the expression of ZAG was consistently reduced in sera and skin of AD patients, suggesting that loss of ZAG may be involved in AD pathogenesis.

ZAG is located in stratum corneum and regulates FLG and TSLP expression in normal human epidermal keratinocytes

Skin barrier abnormalities in AD typically involve altered extracellular lipid composition in the stratum corneum, as well as *FLG* gene mutations (On et al., 2017; Palmer et al., 2006). To evaluate the relationship between ZAG and skin barrier function, we investigated the expression of ZAG and FLG in the skin and in normal human epidermal keratinocytes (NHEKs). In the skin, ZAG expression co-localized to the stratum corneum with LOR and FLG; however, ZAG was not expressed in stratum granulosum, where LOR and FLG showed the strongest staining intensity. Interestingly, AD skin exhibited downregulated expression of ZAG, LOR, and FLG compared with HC skin (Figure 2a). Notably, in stratum corneum of flaky tail (*ft/ft*) mice, the expression of ZAG was reduced (Supplementary Figure S1a online). In NHEKs, the expression of ZAG was higher than T cells, and differentiation of NHEKs in high Ca^{2+} (1.8 mM) concentrations increased *AZGP1* expression (Supplementary Figure S2 online).

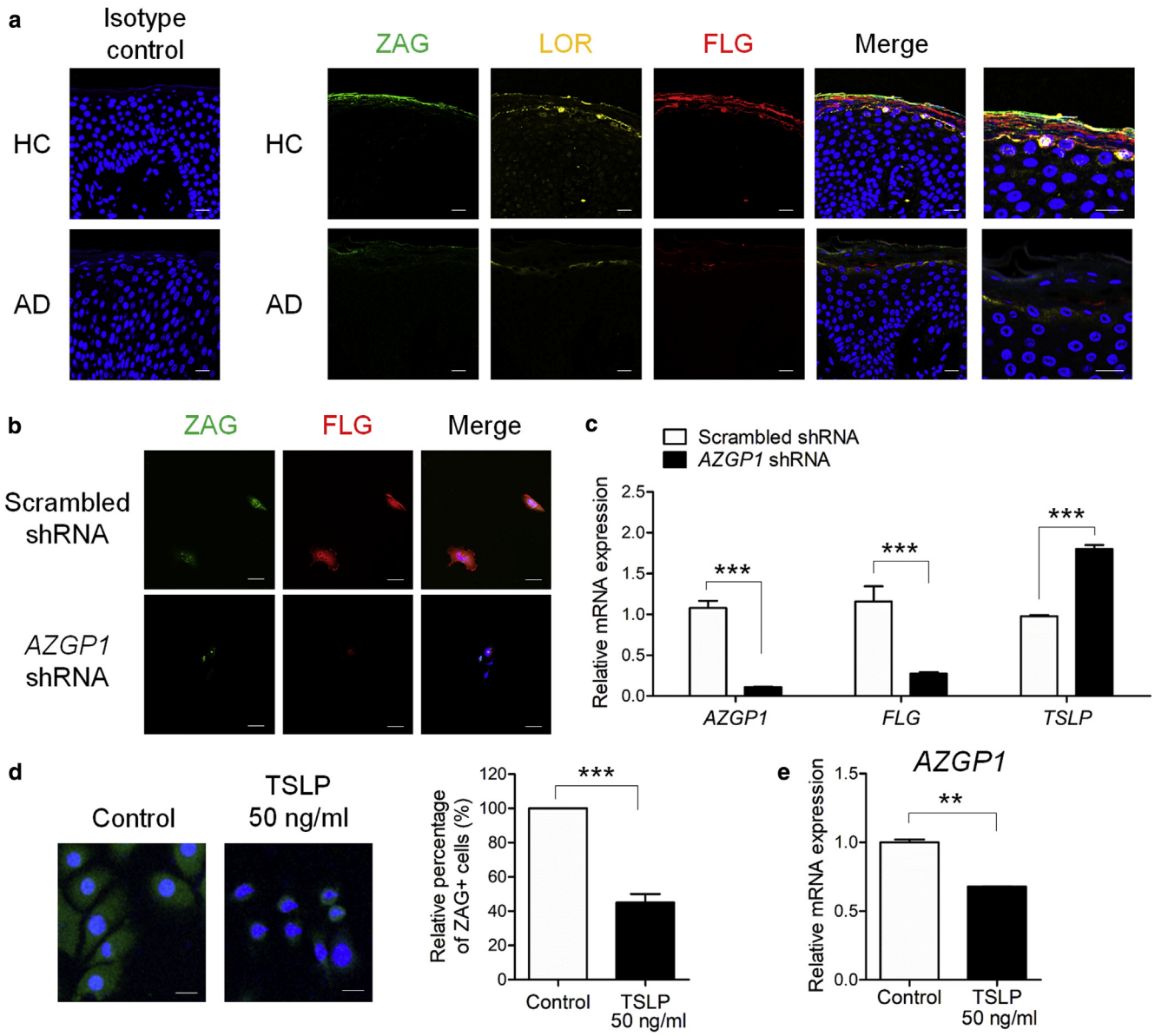

Figure 2. Co-localization of ZAG with skin barrier proteins and regulatory role of ZAG on FLG and TSLP expression in normal human epidermal keratinocytes. (**a**) Immunofluorescence staining of ZAG (green), LOR (yellow), FLG (red), and DAPI (blue) in HC (n = 9) and AD (n = 20) skin samples. (**b**) Immunofluorescence staining of ZAG (green), FLG (red), and DAPI (blue) in scrambled and *AZGP1* shRNA-transfected-normal human epidermal keratinocytes. (**c**) Quantitative real-time PCR analyses of *AZGP1, FLG*, and *TSLP* in scrambled and *AZGP1* shRNA-transfected-normal human epidermal keratinocytes (***$P < 0.001$). (**d**) Immunofluorescence staining of ZAG (green) and DAPI (blue) (***$P < 0.001$). (**e**) Quantitative real-time PCR analyses of *AZGP1* in control and 50 ng/ml TSLP-treated normal human epidermal keratinocytes (**$P < 0.01$). All scale bars = 20 μm. Data are presented as mean ± standard error of the mean. AD, atopic dermatitis; HC, healthy control; shRNA, short hairpin RNA.

Supporting the loss of ZAG in flaky tail mice, knockdown of FLG using short hairpin RNA (shRNA) decreased the expression of *AZGP1* in NHEKs (Supplementary Figure S1b).

We next assessed whether ZAG affects FLG expression by knockdown of ZAG using *AZGP1* shRNA in NHEKs. In comparison with scrambled shRNA-transfected cells, *AZGP1* shRNA-transfected NHEKs showed significantly reduced FLG expression by immunofluorescence staining (Figure 2b) and qRT-PCR (Figure 2c). Furthermore, injection of mice with ZAG induced *Flg*, and injection of anti-ZAG mAb decreased *Flg* expression in normal NC/Nga mouse skin (Supplementary Figure S3a, S3b online). Interestingly, *TSLP*, a T helper type 2–skewing cytokine in AD, was significantly increased in *AZGP1* shRNA-transfected NHEKs (Figure 2c). Furthermore, we evaluated whether TSLP affects ZAG expression and found that TSLP-treated NHEKs showed significant reduction of ZAG at the protein (Figure 2d) and mRNA (Figure 2e) levels. Collectively, ZAG regulates FLG and TSLP and can also be regulated by FLG and TSLP, highlighting its association with skin barrier function and immune homeostasis.

ZAG rescues skin barrier function in AD-induced NC/Nga mice and restores ceramide synthesis

To evaluate the effect of ZAG on skin barrier abnormalities in AD, we applied ZAG topically to AD-induced NC/Nga mice as outlined in Figure 3a. The animals were divided into four

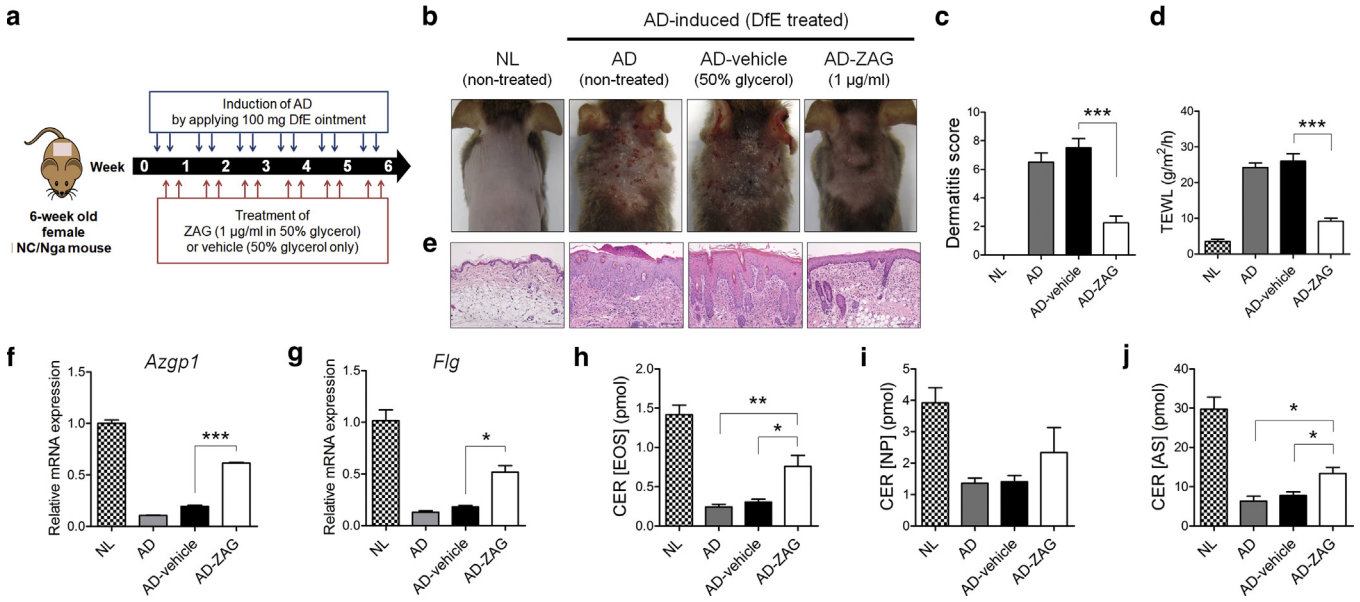

Figure 3. Effect of topical ZAG on AD-induced NC/Nga mice. (**a**) Schematic of experimental design. AD lesions in the mouse model were induced by applying 100 mg DfE ointment for 6 weeks. At the same time, the skin was treated with 1 μg/ml ZAG or vehicle twice a week (n = 5/group). (**b**) Changes in clinical appearance of dorsal skin of mice in NL, AD, AD-vehicle, and AD-ZAG groups. (**c**) Dermatitis scores were plotted for each group after 6 weeks of treatment (***$P < 0.001$). (**d**) Transepidermal water loss was measured on the dorsal skin of mice after 6 weeks of treatment (***$P < 0.001$). (**e**) Hematoxylin and eosin−stained mice skin. Scale bar = 100 μm. Quantitative real-time PCR analyses of (**f**) *Azgp1* and (**g**) *Flg* (*$P < 0.05$). Ultraperformance liquid chromatography-Q/time-of-flight mass spectrometry analysis of (**h**) CER [EOS], (**i**) [NP], and (**j**) [AS] (n = 3/group; *$P < 0.05$, ***$P < 0.001$). Data are presented as mean ± standard error of the mean. AD, atopic dermatitis; AD-ZAG, AD-induced ZAG-treated; CER, ceramide; NL, normal; AD-vehicle, AD-induced vehicle-treated; TEWL, transepidermal water loss.

groups: normal, AD without treatment, AD treated with vehicle, and AD treated with ZAG. Notably, compared to the AD without treatment or AD treated with vehicle groups, the AD treated with ZAG group exhibited less severe AD-like skin lesions (Figure 3b), significant reduction of dermatitis scores (Figure 3c), and lower transepidermal water loss (Figure 3d). Supporting the clinical improvement, hematoxylin and eosin staining of the skin showed decreased epidermal thickness and inflammatory cell infiltration in the AD treated with ZAG group compared to the AD without treatment or AD treated with vehicle group (Figure 3e). Furthermore, mRNA expression levels of *Azagp1* (Figure 3f) and *Flg* (Figure 3g) after AD induction were restored following topical ZAG treatment.

As a previous report suggested that ZAG regulates lipid metabolism (Bao et al., 2005), we evaluated whether topical ZAG treatment affects the synthesis of ceramide (CER), which is a key lipid implicated in AD pathogenesis (Hatano et al., 2005). We found that CER [EOS] was increased in the AD treated with ZAG group compared to the AD without treatment or AD treated with vehicle groups (*$P < 0.05$, **$P < 0.01$; Figure 3h). CER [NP] was also increased in the AD treated with ZAG group compared to the AD without treatment or AD treated with vehicle groups, yet these differences were not statistically significant (Figure 3i). CER [AS] was increased in the AD treated with ZAG group compared to the AD without treatment and AD treated with vehicle groups (*$P < 0.01$; Figure 3j). These results suggest that topical application of ZAG restores the disrupted skin barrier in AD by regulating CER synthesis. However, intradermal injection of recombinant ZAG or anti-ZAG mAb to normal NC/Nga mice did not significantly change CER composition in the skin (Supplementary Figure S3c−S3e), suggesting that ZAG has minimal effects on the normal skin barrier, but is able to repair abnormalities in the skin barrier under AD conditions.

ZAG modulates both local and systemic immune response in AD-induced NC/Nga mice

To investigate whether ZAG affects the immune response, we used qRT-PCR to evaluate mRNA expressions of IL-4, IL-17a, IFN-γ, and Foxp3 in four groups: normal, AD without treatment, AD treated with vehicle, and AD treated with ZAG. The expression levels of *Il-4*, *Il-17a*, and *Ifng* were decreased (Figure 4a−4c), but *Foxp3* expression was significantly increased (Figure 4d) in the AD treated with ZAG group compared with those in the AD without treatment and AD treated with vehicle groups. Notably, we also found reduced *Tslp* expression in the AD treated with ZAG group compared with that in the AD without treatment and AD treated with vehicle groups (Figure 4e).

Next, we evaluated the systemic effects of topical ZAG treatment. The populations of IL-4$^+$CD4$^+$, IL-17$^+$CD4$^+$, and IFN-γ$^+$CD4$^+$ T cells of the AD treated with ZAG group in the lymph nodes (***$P < 0.001$; Figure 4f−4h) and spleen (***$P < 0.001$; Figure 4j−4l) were significantly decreased compared with those in the AD and AD-vehicle groups. On the other hand, the Foxp3$^+$CD4$^+$CD25$^+$ regulatory T population was significantly increased in the AD treated with ZAG group compared with that of the AD without treatment and AD treated with vehicle groups in lymph nodes (***$P < 0.001$; Figure 4i) and spleen (***$P < 0.001$; Figure 4m). We also found that the increased levels of serum total IgE were

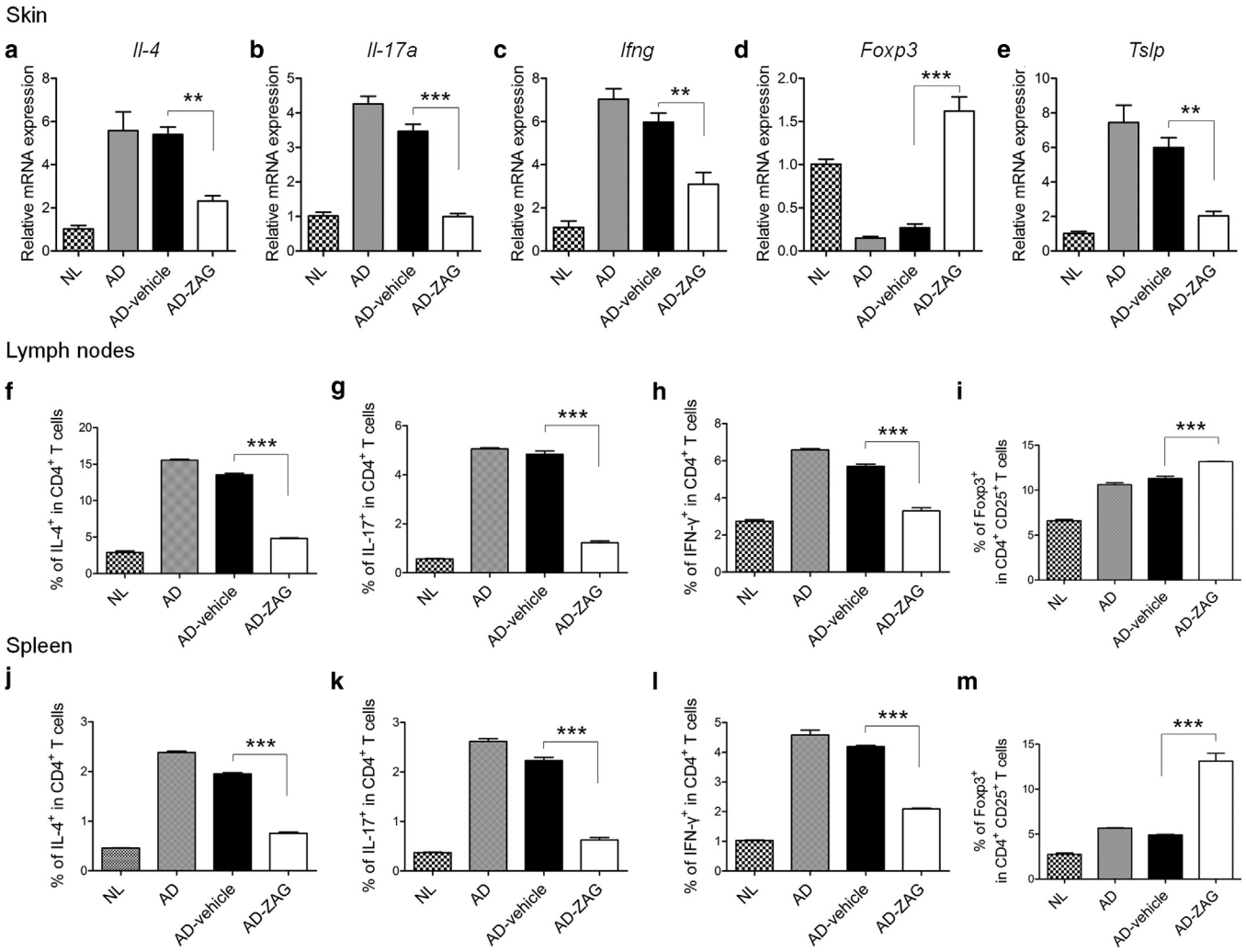

Figure 4. Effect of topical ZAG on local and systemic immune response in AD-induced NC/Nga mice. Quantitative real-time PCR analyses of (**a**) *Il-4*, (**b**) *Il-17a*, (**c**) *Ifng*, (**d**) *Foxp3*, and (**e**) *Tslp* in NL, AD, AD-vehicle, and AD-ZAG groups (**$P < 0.01$, ***$P < 0.001$). Populations of IL-4$^+$ (**f, j**), IL-17$^+$ (**g, k**), and IFN-γ$^+$ cells (**h, l**) in CD4$^+$ T cells and Foxp3$^+$ cells in CD4$^+$CD25$^+$ regulatory T cells (**i, m**) were determined by FACS analysis in lymph nodes (**f**–**i**) and spleen (**j**–**m**; ***$P < 0.001$) from each group. Data are presented as mean ± standard error of the mean of three independent determinations. AD, atopic dermatitis; AD-vehicle, AD-induced vehicle-treated; AD-ZAG, AD-induced ZAG-treated.

significantly suppressed from week 4 in AD treated with ZAG mice compared with those of AD without treatment or AD treated with vehicle mice (Supplementary Figure S4 online).

Anti-inflammatory effect of ZAG on T cells and NHEKs

Next, we evaluated the direct anti-inflammatory effects of ZAG on T cells, macrophages, and NHEKs. Cell viability tests were used to determine the optimal ZAG treatment concentration of 1 μg/ml (data not shown). Flow cytometry analysis showed a decrease of IL-4$^+$CD4$^+$ and IL-17$^+$CD4$^+$ T cells and an increase of Foxp3$^+$CD4$^+$CD25$^+$ regulatory T cells in human AD T cells following ZAG treatment (Supplementary Figure S5a–S5c online). In NHEKs, the increased expression of thymus and activation-regulated cytokine and *TSLP* by TNF-α and IFN-γ was ameliorated in ZAG-treated NHEKs (Supplementary Figure S5d, S5e). Collectively, these results suggest that ZAG exerts direct anti-inflammatory effects on T cells and NHEKs, offering a possible explanation for the local and systemic immunomodulation in ZAG-treated AD mice.

ZAG is related to ADAM17 signaling activation in the skin and T cells

We analyzed the gene expression profiles of lipid metabolism (Figure 5a) and the immune response in human skin (Figure 5b) and T cells (Figure 5c). Upon reduction of ZAG, genes associated with epidermal homeostasis and lipid metabolism were reduced in AD skin compared to HC skin. These genes included *PPARG*, *ADIPOQ*, and *FASN*. In contrast, the expression of *CD36*, *FAS*, *SLC27A4*, and *CPT1A* were increased in human AD skin compared to HC skin, and these changes were confirmed by qRT-PCR (Figure 5d). As expected, AD pathogenesis-related genes, such as *IL-1A*, *IL-4R*, *IL-13*, *IL-17A*, and *TSLP*, were increased in the skin and T cells of AD compared to HC (Figure 5b, 5c). Recently, several reports showed that deficiency of ADAM17 and Notch signaling results in AD (Murthy et al., 2012; Woodring et al., 2018) and that ADAM17 regulates skin barrier and immune responses (Bird, 2012). In agreement with previous reports, we also found that the expression of ADAM17 and NOTCH1

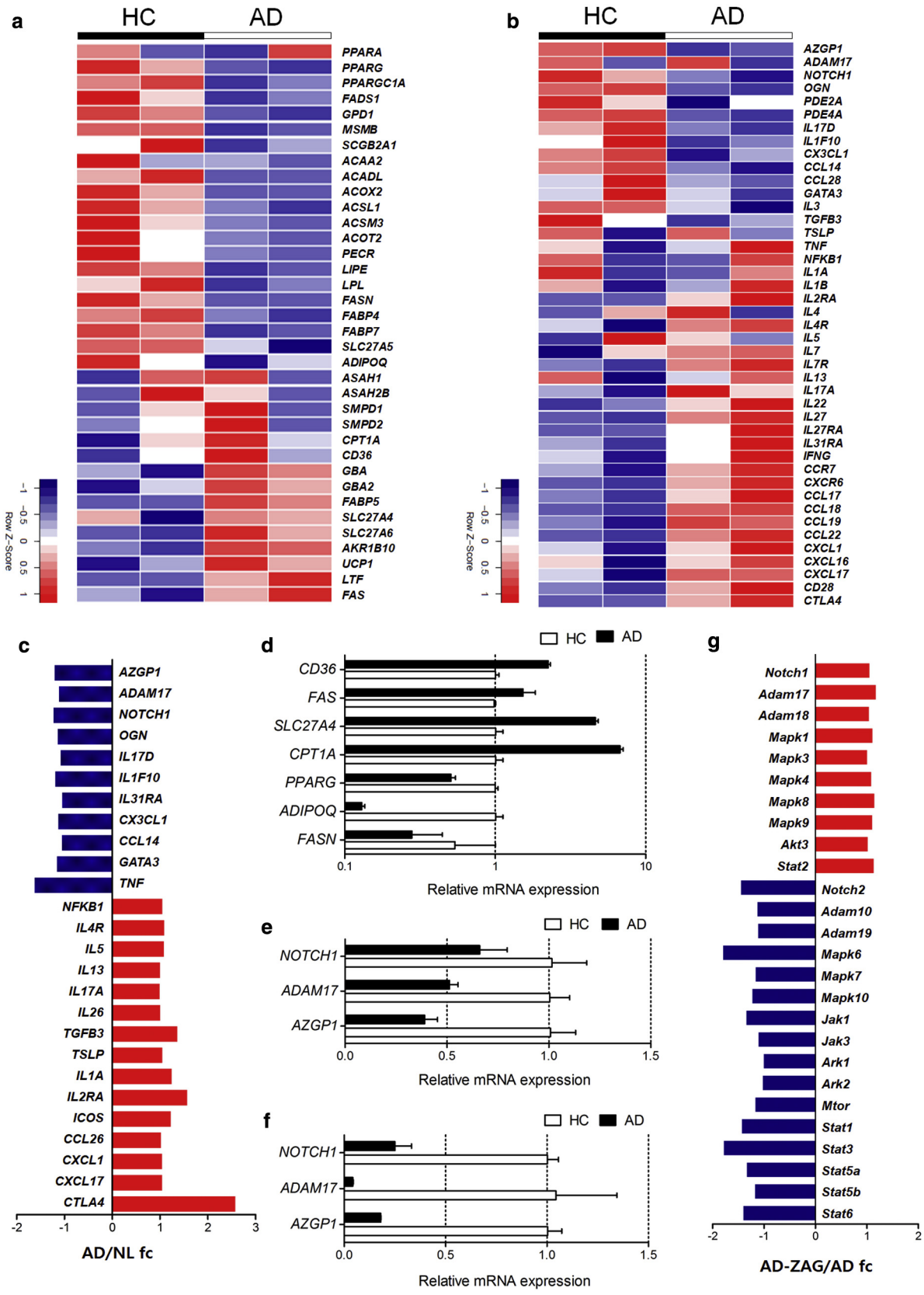

Figure 5. Reduced ADAM17 signaling in AD skin and T cells. Heatmaps of RNA expression levels of lipid metabolism-related genes (**a**) and immune response-related genes (**b**) in human skin. (**c**) mRNA expression levels of immune response-related genes in human T cells. (**d**) Quantitative real-time PCR analyses of lipid metabolism-related genes. Quantitative real-time PCR analyses of AZGP1, ADAM17, and NOTCH1 in human skin (**e**) and T cells (**f**). (**g**) Changes in signaling molecule-related genes between AD-ZAG–treated mouse skin and AD mouse skin. AD, atopic dermatitis; HC, healthy control.

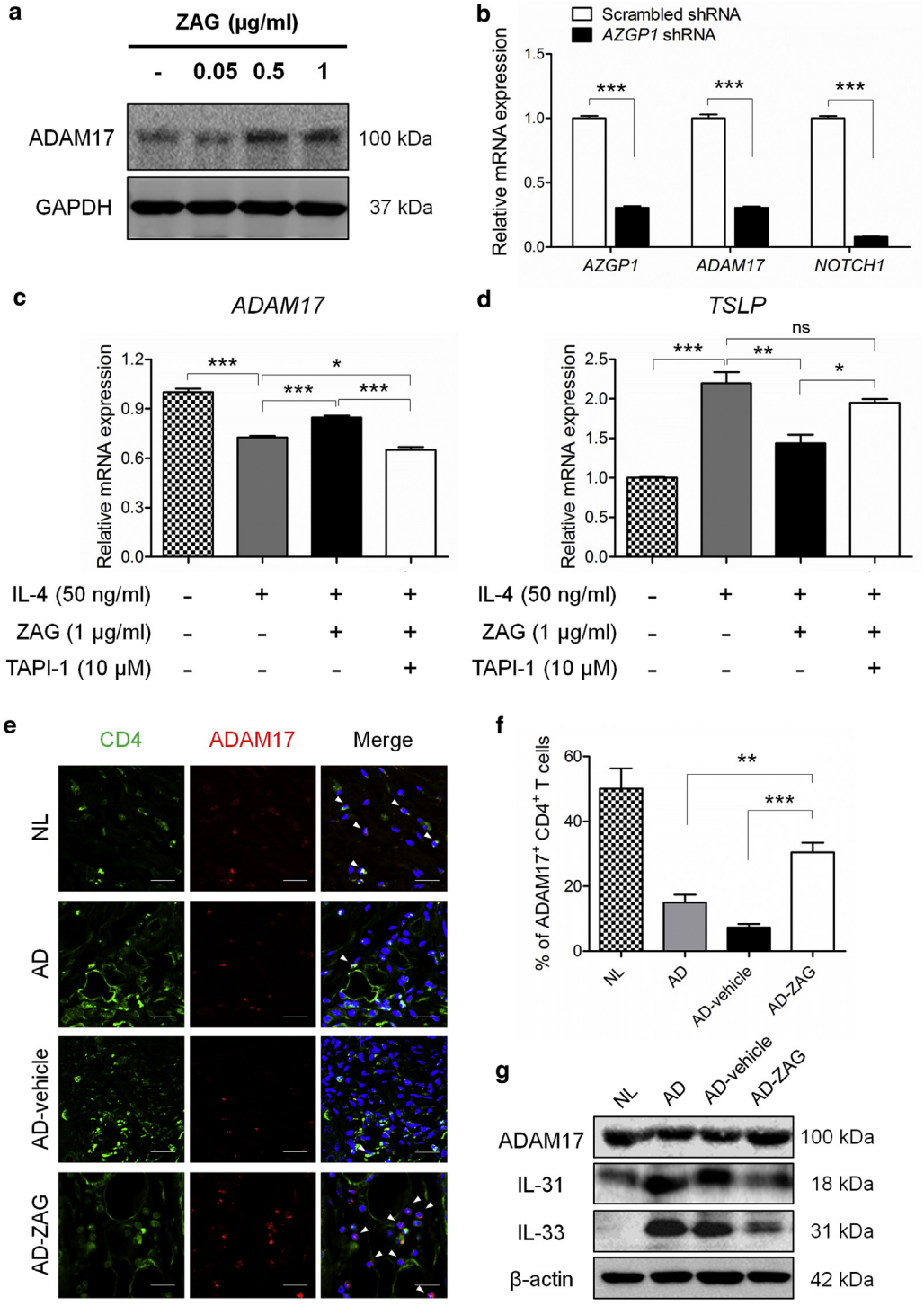

Figure 6. ZAG regulates the expression of ADAM17 in normal human epidermal keratinocytes and AD-ZAG NC/Nga mice. (**a**) Western blots of ADAM17 in ZAG-treated normal human epidermal keratinocytes. (**b**) Quantitative real-time PCR analyses of *ADAM17* and *NOTCH1* in scrambled and *AZGP1* shRNA-transfected normal human epidermal keratinocytes (***$P < 0.001$). *ADAM17* (**c**) and *TSLP* (**d**) mRNA expression with the combined treatment of IL-4, ZAG, and TAPI-1 (ADAM17 inhibitor). (**e**) Immunofluorescence staining of CD4 (green), ADAM17 (red) and DAPI (blue) in the dermis of NL, AD, AD-vehicle, and AD-ZAG groups (n = 3/group). Scale bar = 20 μm. (**f**) Percentage of ADAM17$^+$CD4$^+$ T cells (**$P < 0.01$, ***$P < 0.001$) and (**g**) Western blots of ADAM17, IL-31, and IL-33 in NL, AD, AD-vehicle, and AD-ZAG groups (n = 3/group). Data are presented as mean ± standard error of the mean. AD, atopic dermatitis; AD vehicle, AD-induced vehicle-treated; AD-ZAG, AD-induced ZAG-treated; GAPDH, glyceraldehyde 3-phosphate dehydrogenase; NL, normal; shRNA, short hairpin RNA.

were decreased in both skin and T cells of AD compared to HC (Figure 5b, 5c), and these results were confirmed by qRT-PCR (Figure 5e, 5f). Also, comparison of gene expression profiles between the skin of AD-ZAG and AD mice revealed that topical ZAG application restored ADAM17 and Notch1 expression in AD-induced mice (Figure 5g).

Because levels of ADAM17 and Notch1 were decreased in AD compare with HC and their expression levels were

restored following topical ZAG treatment in mice, we further evaluated the relationship between ADAM17 and ZAG. ADAM17 was increased in NHEKs treated with ZAG (Figure 6a). In addition, knockdown of *AZGP1* using shRNA in NHEKs induced reduction of *ADAM17* and *NOTCH1* compared to transfection with scrambled shRNA, suggesting that ZAG is a regulator of ADAM17 in NHEKs (***$P < 0.001$; Figure 6b). Interestingly, ZAG treatment ameliorated the IL-4-induced decrease of *ADAM17* (***$P < 0.001$; Figure 6c) and increase of *TSLP* in NHEKs (***$P < 0.001$; Figure 6d). Furthermore, treatment with the ADAM17 inhibitor, TAPI-1, reversed the effects of ZAG on NHEKs (*$P < 0.05$, ***$P < 0.001$; Figure 6c, 6d). We also conducted similar experiments using *ADAM17* shRNA-transfected NHEKs. We found that treatment of ZAG did not affect mRNA levels of *TSLP* in *ADAM17* shRNA-transfected NHEKs (Supplementary Figure S6a, S6b online).

We also found that both ZAG and ADAM17 expression was decreased in the stratum corneum (Supplementary Figure S7a online) and that the population of $ZAG^+ADAM17^+CD4^+$ T cells was decreased in the dermis (Supplementary Figure S7b) of AD skin compared to HC skin. Similarly, the population of $ADAM17^+CD4^+$ T cells was reduced in the dermis of AD without treatment and AD treated with vehicle NC/Nga mice compared to the dermis of normal mice. The decreased ADAM17 levels recovered following topical ZAG treatment (Figure 6e, 6f). Decreased expression of ADAM17 in untreated AD and AD treated with vehicle mice and ZAG-induced recovery of ADAM17 in AD treated with ZAG mice were also confirmed by Western blot analysis (Figure 6g). We also detected decreased expression of IL-31 and IL-33, which are related to epidermal skin barrier and inflammation (Di Salvo et al., 2018). Collectively, these data suggest that ZAG may rescue immunological abnormalities in AD via regulation of ADAM17.

DISCUSSION

Previous studies have shown that adipokines modulate immune responses and lipid metabolism in allergic disease (Nagel et al., 2009). ZAG is regulated by adiposity and agents that influence lipolysis and the inflammatory response (Mracek et al., 2010). Recently, AD has been categorized as a member of the systemic disorder spectrum along with cardiovascular diseases and obesity (Brunner et al., 2017). Although the association between AD and obesity remains ambiguous, obesity is prevalent in both pediatric and adult patients with AD (Silverberg et al., 2015; Zhang and Silverberg, 2015). In addition, studying the relationship between AD and lipid metabolism revealed that lipid accumulation and suppression of fatty acid β-oxidation occurred in livers of an AD mouse model (Seino et al., 2012). These findings suggest a possible role for adiposity-related adipokines in AD pathogenesis; however, the effects of adipokines on AD pathogenesis have not been elucidated (Balato et al., 2011; Han et al., 2016; Machura et al., 2013; Nagel et al., 2009).

ZAG was discovered as a biomarker in carcinomas, such as breast cancer, prostate cancer, colorectal cancer, as well as in obesity and diabetes (Dubois et al., 2010; Hassan et al., 2008; Ji et al., 2013; Sidaway, 2017). Here, we implicated ZAG as a biomarker candidate for AD using 2-dimensional difference gel electrophoresis coupled with tandem mass spectrometry analysis. Notably, significant loss of ZAG was observed in the skin, T cells, and sera of AD patients. Furthermore, we demonstrated that ZAG regulates FLG and CER, which are crucial in skin barrier function, and that exogenous ZAG can rescue immune response abnormalities and skin barrier dysfunction in AD through recovery of ADAM17.

Functional mutations in FLG result in skin barrier perturbation, eventually inducing allergic sensitization in patients with AD. Moreover, T helper type 2 cytokines actively downregulate FLG expression in AD lesions, further aggravating allergic inflammation (Howell et al., 2007). Current therapeutic approaches to AD focus mainly on modulation of the dysfunctional barrier and suppression of systemic T helper type 2 inflammation (Pantazi et al., 2018). Treatment methods targeting the dysfunctional barrier are, however, limited, and identification of new AD therapeutic targets that can efficiently improve barrier function is certainly important. In this study, we demonstrated that ZAG was expressed in the skin in the stratum corneum and that knockdown of ZAG resulted in decreased expression of FLG, implying that ZAG is a regulator of FLG in human keratinocytes. These data suggest a possible role for ZAG in skin barrier dysfunction in AD and indicate that modulation of ZAG may be an effective treatment strategy to recover FLG expression and barrier dysfunction in AD.

Therefore, we further addressed the therapeutic efficacy of ZAG. Remarkably, topical treatment of ZAG on AD-induced NC/Nga mice improved both barrier integrity and immunological profiles of AD-like inflammation. Although the molecular weight of ZAG is 41 kDa, evidence suggests that ZAG can penetrate the disrupted skin barrier in AD (Furuse et al., 2002). There have been many reports about ZAG signaling pathways (Ceperuelo-Mallafre et al., 2015; Chang et al., 2014; Kong et al., 2010); yet, a receptor or a signaling pathway for ZAG in keratinocytes or T cells has not been identified. Here, we showed that topical ZAG treatment restored ADAM17 and Notch1 signaling in AD-induced mice. ADAM17 is a regulator of TNF-α (Scheller et al., 2011), and maintains the skin barrier function (Bird, 2012). Recent reports indicated that deficiency of ADAM17 and Notch signaling underlies AD (Murthy et al., 2012; Woodring et al., 2018). Interestingly, the effect of ZAG on the regulation of IL-4–induced TSLP in NHEKs was ameliorated by blockade of ADAM17 signaling, suggesting that ADAM17 is a downstream regulator of ZAG. Based on these results, we suggest that ZAG restores T helper type 2–induced skin barrier abnormalities via ADAM17 signaling and that restoration of skin barrier abnormalities may recover local and systemic immune responses as well. Furthermore, ZAG showed direct anti-inflammatory effects on T cells, macrophages, and NHEKs, potentially contributing to the immunemodulatory effects of topical ZAG treatment. In the future, further research will be necessary to identify the signaling pathways that are involved in the regulation of ADAM17 following ZAG treatment.

In summary, we demonstrated that ZAG modulates both skin barrier function and immune responses of the skin,

highlighting ZAG as a potential therapeutic candidate for AD treatment.

Although various treatment modalities, including topical steroids, moisturizers, and immunotherapy, are currently used to treat AD, more effective and safe treatments are still much needed (Akdis, 2012). Restoration of ZAG via simple topical application may offer a treatment option in AD, as this molecule simultaneously improves skin barrier function, immune response, and inflammation.

MATERIALS AND METHODS

Human sample collections

After obtaining written informed consent, human sera, skin tissues, and peripheral blood mononuclear cells were obtained in accordance with a protocol approved by the Yonsei University College of Medicine Institutional Review Board (4-2013-0624). AD was diagnosed by dermatologists in the Atopic Dermatitis Special Clinic of Severance Hospital (Seoul, Korea) using the Hanifin and Rajka diagnostic criteria. Clinical AD severity was assessed independently and blindly by clinicians using the Eczema Area and Severity Index. All experiments involving humans were performed in adherence with the Declaration of Helsinki. Patient age and sex, Eczema Area and Severity Index, and related sera profiles are listed in Supplementary Table S1 online.

Induction of AD mouse model and topical ZAG treatment

Six-week-old female NC/Nga mice were purchased from SLC Japan (Shizuoka, Japan). The skin barrier was disrupted by applying 200 μl of 4% SDS solution (Sigma-Aldrich, St Louis, MO). After 2 hours, 100 mg of *Dermatophagoides farinae* body extract ointment (Biostir, Kobe, Japan) was topically applied twice a week for 6 weeks to induce AD-like symptoms. Mice were divided into four groups: normal, AD without treatment, AD treated with vehicle, and AD treated with ZAG. Vehicle (50% glycerol) and 1 μg/ml recombinant human ZAG (Biovendor, Brno, Czech Republic) in 50% glycerol was topically applied twice a week for 6 weeks during induction of AD (Figure 3a). All animal experiments were conducted according to the guidelines of the Animal Research Ethics Board of Yonsei University (Seoul, Korea).

CER analysis

For CER extraction, the stratum corneum of NC/Nga mice (n = 3−4 for each group) was collected by tape stripping. Methanol (2 ml) was added to immersed mouse skin patches, and samples were vortexed and then sonicated. Analysis of CER extracts was performed using the AQUITY UPLC system coupled to a Synapt G2-HDMS mass spectrometer (Waters, Milford, MA) equipped with an electron spray ionization source. Detailed description in the Supplementary Materials and Methods online.

Flow cytometry

Single cells were isolated from mouse lymph nodes and spleen using 40-μm mesh sieves. The cells were cultured in the presence of anti-CD3 and anti-CD28 (eBioscience, San Diego, CA) antibodies and then treated with Cell Stimulation Cocktail (plus protein transport inhibitors; eBioscience) at a concentration of 2 μg/ml for 6 hours. After washing with phosphate buffered saline, the cells were labeled with anti-CD4 and anti-CD25 antibodies conjugated with a fluorescent dye (eBioscience). For intracellular labeling, cells were fixed and permeabilized with a cytofix/cytoperm buffer (eBioscience) and labeled with anti−IL-4, anti−IL-17, anti−IFN-γ, and anti−Foxp3 antibodies conjugated with a fluorescent dye. These labeled cells were quantified using a BD LSR Fortessa flow cytometer and analyzed using FlowJo Software (BD Biosciences, Franklin Lake, NJ).

Statistical analyses

Statistical analyses were conducted with GraphPad Prism, version 4.03 (San Diego, CA). All data are representative of two or three independent experiments. Data were analyzed using a one-way analysis of variance, and the significance of the differences was determined using an unpaired *t* test or Tukey-Kramer test. Correlations were determined by calculating Pearson's correlation coefficient. All *P*-values <0.05 were considered statistically significant.

Data availability statement

The microarray data that support the findings of this study have been deposited in National Center for biotechnology Information's Gene Expression Omnibus and are accessible through Gene Expression Omnibus Series accession number GSE124700 for human skin, GSE124701 for human T cell, and GSE124550 for mouse skin data.

ORCIDs

Ji Yeon Noh: http://orcid.org/0000-0002-4158-9443
Jung U Shin: http://orcid.org/0000-0001-5259-6879
Ji Hye Kim: http://orcid.org/0000-0003-2734-1174
Seo Hyeong Kim: http://orcid.org/0000-0002-3720-2509
Bo-Mi Kim: http://orcid.org/0000-0003-3494-6956
Young Hwan Kim: http://orcid.org/0000-0003-3478-8839
Semin Park: http://orcid.org/0000-0002-1355-2408
Tae-Gyun Kim: http://orcid.org/0000-0002-2116-4579
Kyong-Oh Shin: http://orcid.org/0000-0002-7174-1311
Kyungho Park: http://orcid.org/0000-0002-1552-9914
Kwang Hoon Lee: http://orcid.org/0000-0002-4361-1819

CONFLICT OF INTEREST

The authors state no conflict of interest.

ACKNOWLEDGEMENTS

This study was supported by grants from the Korean Health Technology R & D Project, Ministry of Health, Welfare and Family Affairs, Republic of Korea (HI13C0010).

SUPPLEMENTARY MATERIAL

Supplementary material is linked to the online version of the paper at www.jidonline.org, and at https://doi.org/10.1016/j.jid.2019.01.023.

REFERENCES

Akdis CA. Therapies for allergic inflammation: refining strategies to induce tolerance. Nat Med 2012;18:736−49.

Balato N, Nino M, Patruno C, Matarese G, Ayala F. "Eczemas" and leptin. Dermatitis 2011;22:320−3.

Bao Y, Bing C, Hunter L, Jenkins JR, Wabitsch M, Trayhurn P. Zinc-alpha2-glycoprotein, a lipid mobilizing factor, is expressed and secreted by human (SGBS) adipocytes. FEBS Lett 2005;579:41−7.

Bieber T. Atopic dermatitis. N Engl J Med 2008;358:1483−94.

Bing C, Mracek T, Gao D, Trayhurn P. Zinc-alpha2-glycoprotein: an adipokine modulator of body fat mass? Int J Obes (Lond) 2010;34:1559−65.

Bird L. ADAM17—gatekeeper of the skin barrier. Nat Rev Immunol 2012;12:154.

Boguniewicz M, Leung DY. Atopic dermatitis: a disease of altered skin barrier and immune dysregulation. Immunol Rev 2011;242:233−46.

Brunner PM, Silverberg JI, Guttman-Yassky E, Paller AS, Kabashima K, Amagai M, et al. Increasing comorbidities suggest that atopic dermatitis is a systemic disorder. J Invest Dermatol 2017;137:18−25.

Ceperuelo-Mallafre V, Ejarque M, Duran X, Pachon G, Vazquez-Carballo A, Roche K, et al. Zinc-alpha2-glycoprotein modulates AKT-dependent insulin signaling in human adipocytes by activation of the PP2A phosphatase. PLoS One 2015;10:e0129644.

Chang L, Tian X, Lu Y, Jia M, Wu P, Huang P. Alpha-2-glycoprotein 1(AZGP1) regulates biological behaviors of LoVo cells by down-regulating mTOR signaling pathway and endogenous fatty acid synthesis. PLoS One 2014;9:e99254.

Chen SH, Arany I, Apisarnthanarax N, Rajaraman S, Tyring SK, Horikoshi T, et al. Response of keratinocytes from normal and psoriatic epidermis to interferon-gamma differs in the expression of zinc-alpha(2)-glycoprotein and cathepsin D. FASEB J 2000;14:565–71.

Di Salvo E, Ventura-Spagnolo E, Casciaro M, Navarra M, Gangemi S. IL-33/IL-31 axis: a potential inflammatory pathway. Mediators Inflamm 2018;2018:3858032.

Dubois V, Delort L, Mishellany F, Jarde T, Billard H, Lequeux C, et al. Zinc-alpha2-glycoprotein: a new biomarker of breast cancer? Anticancer Res 2010;30:2919–25.

Furuse M, Hata M, Furuse K, Yoshida Y, Haratake A, Sugitani Y, et al. Claudin-based tight junctions are crucial for the mammalian epidermal barrier: a lesson from claudin-1-deficient mice. J Cell Biol 2002;156:1099–111.

Guler N, Kirerleri E, Ones U, Tamay Z, Salmayenli N, Darendeliler F. Leptin: does it have any role in childhood asthma? J Allergy Clin Immunol 2004;114:254–9.

Hale LP. Zinc alpha-2-glycoprotein regulates melanin production by normal and malignant melanocytes. J Invest Dermatol 2002;119:464–70.

Han B, Wu WH, Bae JM, Son SJ, Lee JH, Han TY. Serum leptin and adiponectin levels in atopic dermatitis (AD) and their relation to disease severity. J Am Acad Dermatol 2016;75:629–31.

Hassan MI, Waheed A, Yadav S, Singh TP, Ahmad F. Zinc alpha 2-glycoprotein: a multidisciplinary protein. Mol Cancer Res 2008;6:892–906.

Hatano Y, Terashi H, Arakawa S, Katagiri K. Interleukin-4 suppresses the enhancement of ceramide synthesis and cutaneous permeability barrier functions induced by tumor necrosis factor-alpha and interferon-gamma in human epidermis. J Invest Dermatol 2005;124:786–92.

Howell MD, Kim BE, Gao P, Grant AV, Boguniewicz M, Debenedetto A, et al. Cytokine modulation of atopic dermatitis filaggrin skin expression. J Allergy Clin Immunol 2007;120:150–5.

Ji D, Li M, Zhan T, Yao Y, Shen J, Tian H, et al. Prognostic role of serum AZGP1, PEDF and PRDX2 in colorectal cancer patients. Carcinogenesis 2013;34:1265–72.

Kong B, Michalski CW, Hong X, Valkovskaya N, Rieder S, Abiatari I, et al. AZGP1 is a tumor suppressor in pancreatic cancer inducing mesenchymal-to-epithelial transdifferentiation by inhibiting TGF-beta-mediated ERK signaling. Oncogene 2010;29:5146–58.

Machura E, Szczepanska M, Ziora K, Ziora D, Swietochowska E, Barc-Czarnecka M, et al. Evaluation of adipokines: apelin, visfatin, and resistin in children with atopic dermatitis. Mediators Inflamm 2013;2013:760691.

Malik K, Heitmiller KD, Czarnowicki T. An update on the pathophysiology of atopic dermatitis. Dermatol Clin 2017;35:317–26.

Mracek T, Ding Q, Tzanavari T, Kos K, Pinkney J, Wilding J, et al. The adipokine zinc-alpha2-glycoprotein (ZAG) is downregulated with fat mass expansion in obesity. Clin Endocrinol (Oxf) 2010;72:334–41.

Murthy A, Shao YW, Narala SR, Molyneux SD, Zuniga-Pflucker JC, Khokha R. Notch activation by the metalloproteinase ADAM17 regulates myeloproliferation and atopic barrier immunity by suppressing epithelial cytokine synthesis. Immunity 2012;36:105–19.

Nagel G, Koenig W, Rapp K, Wabitsch M, Zoellner I, Weiland SK. Associations of adipokines with asthma, rhinoconjunctivitis, and eczema in German schoolchildren. Pediatr Allergy Immunol 2009;20:81–8.

On HR, Lee SE, Kim SE, Hong WJ, Kim HJ, Nomura T, et al. Filaggrin mutation in korean patients with atopic dermatitis. Yonsei Med J 2017;58:395–400.

Palmer CN, Irvine AD, Terron-Kwiatkowski A, Zhao Y, Liao H, Lee SP, et al. Common loss-of-function variants of the epidermal barrier protein filaggrin are a major predisposing factor for atopic dermatitis. Nat Genet 2006;38:441–6.

Pantazi E, Valenza G, Hess M, Hamad B. The atopic dermatitis market. Nat Rev Drug Discov 2018;17:237–8.

Russell ST, Tisdale MJ. Role of beta-adrenergic receptors in the anti-obesity and anti-diabetic effects of zinc-alpha2-glycoprotien (ZAG). Biochim Biophys Acta 2012;1821:590–9.

Sanchez LM, Chirino AJ, Bjorkman P. Crystal structure of human ZAG, a fat-depleting factor related to MHC molecules. Science 1999;283:1914–9.

Saucillo DC, Gerriets VA, Sheng J, Rathmell JC, Maciver NJ. Leptin metabolically licenses T cells for activation to link nutrition and immunity. J Immunol 2014;192:136–44.

Scheller J, Chalaris A, Garbers C, Rose-John S. ADAM17: a molecular switch to control inflammation and tissue regeneration. Trends Immunol 2011;32:380–7.

Seino S, Tanaka Y, Honma T, Yanaka M, Sato K, Shinohara N, et al. Atopic dermatitis causes lipid accumulation in the liver of NC/Nga mouse. J Clin Biochem Nutr 2012;50:152–7.

Shore SA, Schwartzman IN, Mellema MS, Flynt L, Imrich A, Johnston RA. Effect of leptin on allergic airway responses in mice. J Allergy Clin Immunol 2005;115:103–9.

Shore SA, Terry RD, Flynt L, Xu A, Hug C. Adiponectin attenuates allergen-induced airway inflammation and hyperresponsiveness in mice. J Allergy Clin Immunol 2006;118:389–95.

Sidaway P. Prostate cancer: AZGP1 expression predicts favourable outcomes. Nat Rev Urol 2017;14:391.

Silverberg JI, Becker L, Kwasny M, Menter A, Cordoro KM, Paller AS. Central obesity and high blood pressure in pediatric patients with atopic dermatitis. JAMA Dermatol 2015;151:144–52.

Suarez-Farinas M, Tintle SJ, Shemer A, Chiricozzi A, Nograles K, Cardinale I, et al. Nonlesional atopic dermatitis skin is characterized by broad terminal differentiation defects and variable immune abnormalities. J Allergy Clin Immunol 2011;127:954–64.e1-4.

Tang CH, Chiu YC, Tan TW, Yang RS, Fu WM. Adiponectin enhances IL-6 production in human synovial fibroblast via an AdipoR1 receptor, AMPK, p38, and NF-kappa B pathway. J Immunol 2007;179:5483–92.

Tilg H, Moschen AR. Adipocytokines: mediators linking adipose tissue, inflammation and immunity. Nat Rev Immunol 2006;6:772–83.

Woodring T, Kobayashi T, Kim D, Nagao K. ADAM17 deficient mice model the transcriptional signature of human atopic dermatitis. J Invest Dermatol 2018;138:2283–6.

Zahid H, Miah L, Lau AM, Brochard L, Hati D, Bui TT, et al. Zinc-induced oligomerization of zinc alpha2 glycoprotein reveals multiple fatty acid-binding sites. Biochem J 2016;473:43–54.

Zhang A, Silverberg JI. Association of atopic dermatitis with being overweight and obese: a systematic review and metaanalysis. J Am Acad Dermatol 2015;72:606–16.e1-4.

SUPPLEMENTARY MATERIALS AND METHODS

2-Dimensional difference gel electrophoresis

2-Dimensional difference gel electrophoresis was performed in the dark. Fifty micrograms of each sample (HC, n = 15 and AD, n = 40) and a pooled internal standard were cross-labeled with 400 pmol Cy3, Cy5, and Cy2 dye (GE Healthcare, Madison, WI). The labeled mixtures were combined and loaded for first-dimension separation by isoelectric focusing, followed by second-dimension separation. Next, the gels were successively subjected to scanning, spot picking, in-gel digestion, and spotting onto matrix-assisted laser desorption ionization target plates. Finally, spot image analyses and spot selection were performed, and targeted spots were identified by tandem mass spectrometry.

Matrix-assisted laser desorption/ionization–time of flight tandem mass spectrometry

Protein spots were excised from gels with a sterile scalpel, placed into microfuge tubes, and digested with trypsin (Promega, Madison, WI). The peptides were concentrated with POROS R2 and Oligo R3 columns (Applied Biosystems, Foster City, CA). Matrix-assisted laser desorption ionization–time of flight mass spectrometry was performed on a 4800 MALDI-TOF/TOF Analyzer (Applied Biosystems) equipped with a 355-nm Nd:YAG laser. The pressure in the time of flight analyzer was approximately 7.6e-07 Torr. The mass spectra were obtained with the reflectron mode, an accelerating voltage of 20 kV, the sum of 500 laser pulses, and calibration with the 4700 calibration mixture (Applied Biosystems). Data Explorer 4.4 (PerSeptive Biosystems, Framingham, MA) was used for data acquisition and extraction of the monoisotopic masses.

Mascot database search

The mascot algorithm (Matrix Science, Boston, MA) was used to identify peptide sequences present in a protein sequence database (National Center for Biotechnology Information nr database downloaded on June 30, 2014). The database was searched with the following parameters: taxonomy = *Homo sapiens*, fixed modification = carboxyamidomethylated (+57) at cysteine residues, variable modification = oxidized (+16) at methionine residues, maximum allowed missed cleavage = 1, and MS tolerance = 100 ppm.

ELISA

A human ZAG ELISA kit (BioVendor) was used to determine the levels of ZAG in human sera of HC (n = 36) and AD patients (n = 90) following the manufacturer's instructions. To determine cytokine concentration, the following kits were used: human thymus and activation-regulated cytokine (R&D Systems, Minneapolis, MN), mouse IL-6, mouse IL-4, and mouse IL-13 (eBioscience, San Diego, CA). Concentration of total IgE was measured using mouse-IgE (BioLegend, San Diego, CA).

Microarray analysis

Pooled total RNA from human HC (n = 6) and AD (n = 6) skin and human HC (n = 10) and AD (n = 16) T cells were amplified and purified using the TargetAmp-Nano labeling kit for Illumina Expression BeadChip (EPICENTRE, Madison, WI) to obtain biotinylated cRNA according to the manufacturer's instructions. After purification, labeled cRNA samples were hybridized to Human HT-12 v4.0 Expression BeadChips (Illumina, San Diego, CA) for 16 hours at 58°C. Array signals were detected using Amersham Fluorolink streptavidin-Cy3 (GE Healthcare Biosciences, Little Chalfont, UK). Arrays were scanned with a confocal Illumina bead array reader. Raw data were extracted using software (Illumina GenomeStudio, version 2011.1; Gene Expression Module, version 1.9.0). Array probes were logarithmically transformed and normalized using the quantile method. Results of the microarray data for skin analysis and visualization of differentially expressed genes were conducted using Rstudio, version 1.0.143 (www.rstudio.com). Results of the microarray analysis for T cells are given as fold-change.

For mouse skin, the Affymetrix (Santa Clara, CA) whole transcript expression array process was executed (GeneChip Whole Transcript PLUS reagent kit). The cDNA was synthesized using the GeneChip WT (Whole Transcript) amplification kit. The sense cDNA was then fragmented and biotin-labeled with terminal deoxynucleotidyl transferase using the GeneChip WT terminal labeling kit. Labeled target DNA was hybridized to the Affymetrix GeneChip Mouse 2.0 ST array at 45°C for 16 hours. Hybridized arrays were washed and stained on a GeneChip Fluidics Station 450 and scanned on a GCS3000 scanner (Affymetrix). Signal values were computed using the Affymetrix GeneChip Command Console software. Raw data were extracted automatically via an Affymetrix data extraction protocol using the Affymetrix GeneChip Command Console software. Data were summarized and normalized using the robust multi-average method of the Affymetrix Expression Console software. We exported the results using gene level robust multi-average analysis and analyzed the differentially expressed genes.

The data discussed in this publication have been deposited in the National Center for Biotechnology Information's Gene Expression Omnibus and are accessible through Gene Expression Omnibus Series accession number GSE124700 for human skin (https://www.ncbi.nlm.nih.gov/geo/query/acc.cgi?acc=GSE124700), GSE124701 for human T cell (https://www.ncbi.nlm.nih.gov/geo/query/acc.cgi?acc=GSE124701), and GSE 124550 for mouse skin data (https://www.ncbi.nlm.nih.gov/geo/query/acc.cgi?acc=GSE124550).

qRT-PCR

Skin samples were homogenized using a Precellys 24 homogenizer (Bertin Technologies, Montigny-Le-Bretonneux, France) and human T cells and NHEKs were harvested. Total RNA was extracted using a RNeasy Plus mini kit (Qiagen, Hilden, Germany) following the manufacturer's instructions, and cDNA was generated using a Veriti thermal cycler (Applied Biosystems). Then, qRT-PCR was performed at least twice for each sample using 2 μl of cDNA supplemented with the appropriate primers (Applied Biosystems) and a StepOnePlus PCR system (Applied Biosystems). The mRNA expression was calculated using the $2^{-\Delta\Delta CT}$ method. The primer information for qRT-PCR is listed in Supplementary Table S2 online.

Immunohistochemical staining

Paraffinized sections for human HC and AD skin were rehydrated and blocked with 5% bovine serum albumin

(Sigma-Aldrich, St Louis, MO) for 1 hour at room temperature. Sections were incubated overnight at 4°C with 1:100 diluted anti-ZAG antibody (Abcam, Cambridge, MA) and then washed with 0.1% phosphate buffered saline-Tween-20 buffer. DAB^+ staining was performed using an EnVision G|2 Doublestain System, Rabbit/Mouse (DAB+/Permanent Red) kit (Dako, Glostrup, Denmark) and counterstained with hematoxylin. Images were acquired using microscopy (Olympus Corp, Tokyo, Japan), and relative density was analyzed using ImageJ software.

Immunofluorescence staining

Paraffinized skin sections were deparaffinized and antigen retrieval was performed. Samples were then incubated overnight at 4°C with 1:100 diluted primary antibodies followed by incubation with a fluorescently labeled secondary antibody for 2 hours at room temperature. Finally, the tissue was mounted using VECTASHIELD mounting medium (Vector Laboratories, Burlingame, CA) and observed under a fluorescent microscope. Images were acquired using confocal microscopy (Zeiss ZEN LSM 780; Zeiss, Thornwood, NY), and mean fluorescence intensity and cell number were measured by Zeiss ZEN software. The following antibodies were used: anti-human ZAG (Santa Cruz Biotechnology, Dallas, TX), anti-mouse ZAG (Santa Cruz Biotechnology), anti-human FLG (Abcam), anti-human LOR (Abcam), anti-mouse FLG (Abcam), anti-human CD4 (Bioss, Woburn, MA), anti-mouse CD4 (Abcam), and anti-ADAM17 (Abcam).

Flaky tail (ft/ft) mouse model

Six-week-old female homozygous flaky tail mice (*a/a ma ft/ma ft/J*, n = 5), which carry double-homozygous *ft* and *ma* mutations, were raised in an air-conditioned specific pathogen-free room maintained at 24°C ± 2°C and 55% ± 15% humidity. All experimental procedures were approved by the Animal Research Ethics Board of Yonsei University (Seoul, Korea). C57BL/6J (wild-type) mice (n = 5) were used as control mice.

Knockdown of *AZGP1* using shRNA

NHEKs (Gibco, Carlsbad, CA) were cultured in EpiLife medium (Gibco) with growth supplement (HKGS; Gibco). For differentiation, the Ca^{2+} concentration was increased from 60 μM to 1.8 mM. Mission pLKO.1-puro lentivirus vector and non-mammalian scrambled shRNA control (SHC002) were purchased from Sigma-Aldrich and *AZGP1* shRNA (TRCN 0000061359), *FLG* shRNA (TRCN 0000083681), and *ADAM17* shRNA (TRCN0000052172) were generated. Transfection was performed using Lipofectamine 3000 (Invitrogen, ThermoFisher Scientific, Waltham, MA) according to the manufacturer's instructions. NHEKs (passage 3–4) were grown to 70–80% confluence in six-well plates. NHEKs were transfected with either 2 μg shRNA or a scrambled shRNA control for 3 days. Next, the culture medium was replaced with fresh complete medium containing 1 μg/ml of puromycin for selection. The cells were incubated for 1–2 weeks at 37°C in a humidified incubator with 5% CO_2.

Intradermal ZAG and anti-ZAG injection

Six-week-old female NC/Nga mice were purchased from SLC Japan (Shizuoka, Japan). The back hair on these mice was removed 1 day before the experiment began. Mice were divided into three groups: Control, ZAG, and anti-ZAG. The ZAG group was injected with 0.4 μg/ml of ZAG (Biovendor) per day. The anti-ZAG group was injected with 0.5 mg/kg anti-ZAG mAb (Santa Cruz Biotechnology) per day, and the control group was injected with 50 μl of phosphate buffered saline per day.

Dermatitis scoring

The severity of dermatitis in the mice was evaluated once a week, just before each elicitation. The development of erythema/hemorrhage, scarring/dryness, edema, or excoriation/erosion was scored as 0 (none), 1 (mild), 2 (moderate), and 3 (severe). The sum of the individual scores was considered (Yamamoto et al., 2007).

Measurement of transepidermal water loss

The transepidermal water loss was measured on the skin of the shaved backs of mice with a Tewameter TM210 (Courage and Khazaka, Cologne, Germany). For measurement, the mice were anesthetized in a room maintained at 24°C ± 2°C and 55% ± 15% humidity.

Hematoxylin and eosin staining

Skin from NC/Nga mice was collected and fixed in 4% paraformaldehyde for 24 hours. Paraffin-embedded sections were made and stained with hematoxylin and eosin (Sigma-Aldrich) using standard procedures.

CER analysis

For CER extraction, the stratum corneum of NC/Nga mice was collected by tape stripping. Methanol (2 ml) was added to immersed mouse skin patches, which were vortexed and then sonicated for 10 minutes at room temperature. Then, the separated methanol fraction was collected and dried under nitrogen gas at 35°C. A solid-phase extraction process using aminopropyl cartridges (NH2, 100 mg, 1 ml) was performed to separate and purify CERs. Solid-phase extraction cartridges were preconditioned with 2 ml of hexane. The redissolved (200 μl of 11:1 hexane/isopropanol, v/v) extract was loaded in the NH2 cartridge and washed with 2 ml of hexane. CERs were eluted with 2 ml of a hexane/methanol/chloroform mixture (80:10:10, v/v/v). The eluted fraction was dried and dissolved in 200 μl of isopropanol/chloroform (50:50, v/v).

For ultra-performance liquid chromatography-Q/time of flight mass spectrometry, analysis of CER extracts was performed using the AQUITY UPLC system coupled to a Synapt G2-HDMS mass spectrometer (Waters) equipped with an electron spray ionization source. Chromatographic separation was performed with mobile phase conditions of 20 mM ammonium formate pH 5 and methanol on a BEH C18 shield column (1.8 μm; 2.1 mm × 100 mm; Waters). A linear gradient system, starting with 70% mobile phase and gradually increasing to 100% mobile phase, was used. The mass spectrometry conditions were optimized as follows: capillary voltage of 2 kV and 1 kV, cone voltage of 40 eV, source temperature of 120°C and 100°C, cone gas and desolvation gas flow rate of 50 l/h and 900 l/h, and acquisition mass range of 50 to 1,200 m/z for both ionization modes. The tandem mass spectrometry spectra were acquired in the data-dependent acquisition mode with a survey scan at 0.2 second and subsequent tandem mass

spectrometry scans of the three most abundant precursor ions every 0.2 second.

Western blot

NHEKs treated with ZAG and skin samples obtained from normal, AD without treatment, AD treated with vehicle, and AD treated with ZAG mice (n = 5 each) were lysed in pro-prep lysis buffer (Intron, Seoul, Korea), and cellular protein concentrations were determined with a copper (II) sulphate in bicinchoninic acid solution (Sigma-Aldrich). Cell extracts were electrophoresed on 10% or 12% SDS-PAGE and were transferred onto nitrocellulose membranes (GE Healthcare Amersham, Piscataway, NJ) with Tris buffer (0.025 mol/l Tris-HCl, 0.192 mol/l glycine, and 20% MeOH). Membranes were blocked with 5% skim milk in TBS-Tween-20 for 1 hour at room temperature; washed; incubated with specific antibodies for human/mouse-ADAM17, mouse IL-31, and mouse IL-33 (Abcam) overnight at 4°C; washed; and then incubated with horseradish peroxidase–conjugated anti-mouse or anti-rabbit secondary antibodies (Santa Cruz Biotechnology) for 1 hour at room temperature. Detection was performed with enhanced chemiluminescent detection reagents (Santa Cruz Biotechnology) according to the manufacturer's protocol. Glyceraldehyde 3-phosphate dehydrogenase or β-actin (Santa Cruz Biotechnology) were used as the protein loading control. Three independent experiments were performed with nearly identical results, and representative data are shown.

Cell culture and stimulation

NHEKs were purchased from Gibco. NHEKs were treated with 50 ng/ml TSLP (R&D) or 50 ng/ml TNF-α and IFN-γ (R&D) or 50 ng/ml IL-4 (R&D) for 12 hours or 24 hours depends on the experiments. Then, 1 μg/ml of ZAG (Biovendor), with or without TAPI-1 (Selleckchem, Houston, TX), was added for 6 hours or 24 hours. Human T cells were sorted by magnetic-activated cell sorting using the human Pan T Cell Isolation Kit (Miltenyi Biotec, Bergisch Gladbach, Germany) from human peripheral blood mononuclear cells, according to the manufacturer's instructions. For human T-cell stimulation, cells were treated with 50 ng/ml IL-2 (eBioscience) for 24 hours.

REFERENCE

Yamamoto M, Haruna T, Yasui K, et al. A novel atopic dermatitis model induced by topical application with dermatophagoides farinae extract in NC/Nga mice. Allergol Int 2007;56:139–48.

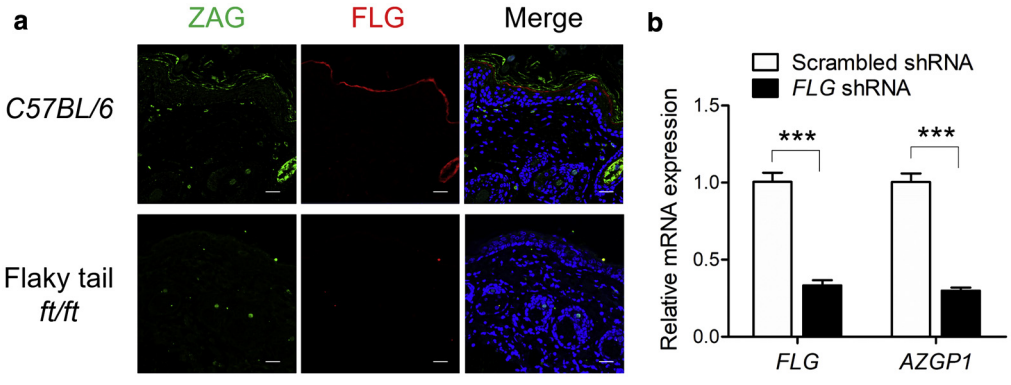

Supplementary Figure S1. Relationship between ZAG and FLG in flaky tail mice and normal human epidermal keratinocytes. (**a**) Immunofluorescence staining of ZAG (green), FLG (red) and DAPI (blue) in the epidermis of 6-week-old wild-type C57BL/6 and flaky tail mice (n = 5/group). Scale bar = 20 μm. (**b**) Quantitative real-time polymerase chain reaction analyses of *FLG* and *AZGP1* in scrambled and *FLG* shRNA-transfected normal human epidermal keratinocytes (***$P < 0.001$). shRNA, short hairpin RNA.

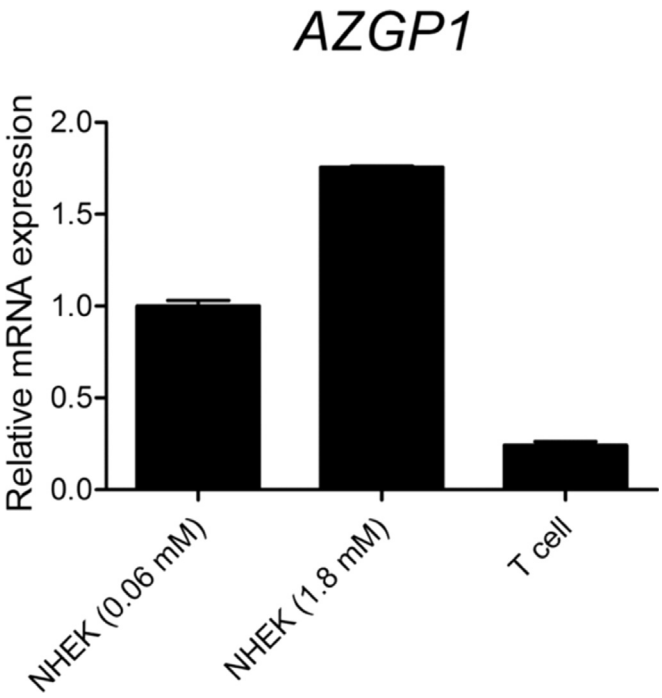

Supplementary Figure S2. *AZGP1* mRNA expression in NHEKs and human T cells. Expression of *AZGP1*, the ZAG coding gene, in NHEKs and human T cells. NHEKs were grown in low (0.06 mM) or high (1.8 mM) Ca^{2+} medium before analysis. NHEK, normal human epidermal keratinocyte.

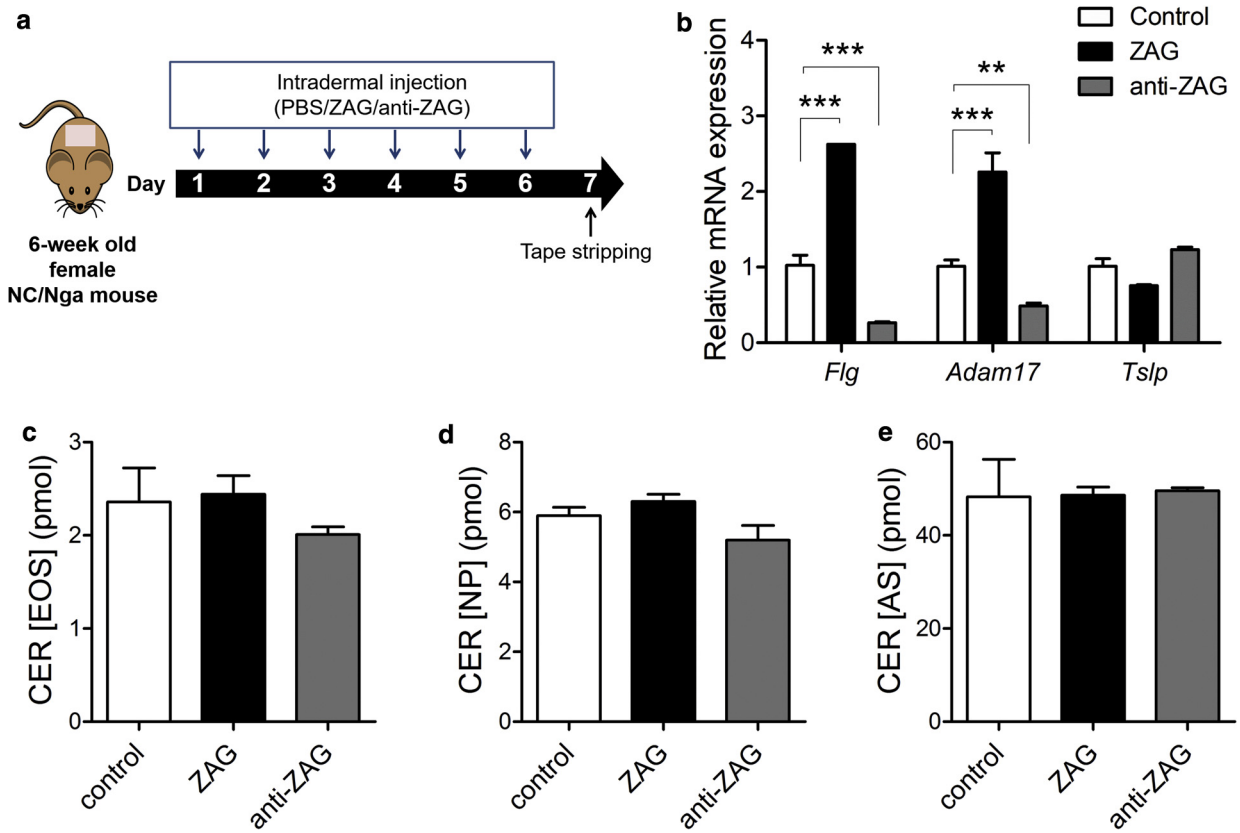

Supplementary Figure S3. Effect of ZAG and anti-ZAG mAb treatment in NC/Nga mice. (**a**) Schematic of experimental design. NC/Nga mice were intradermally injected with PBS (Control), ZAG, or anti-ZAG mAb (n = 3/group). (**b**) *FLG*, *ADAM17*, and *TSLP* mRNA expression levels were determined using quantitative real-time PCR (**$P < 0.01$, ***$P < 0.001$). (**c**–**e**) Ultra-performance liquid chromatography-Q/time of flight mass spectrometry analysis of (**c**) CER [EOS], (**d**) CER [NP], and (**e**) CER [AS] levels in stratum corneum obtained from skin-tape stripping of control, ZAG-, and anti–ZAG-treated mice. CER, ceramide; PBS, phosphate-buffered saline.

Supplementary Figure S4. The increase in total IgE levels was attenuated by topical ZAG treatment in AD-induced NC/Nga mice. Mice sera were obtained weekly from retro-orbital blood samples following induction of AD. Serum IgE levels were measured by ELISA (n = 5/group, $^{**}P < 0.01$, $^{***}P < 0.001$ for AD-vehicle vs. AD-ZAG). AD, atopic dermatitis; AD-vehicle, AD-induced vehicle-treated; AD-ZAG, AD-induced ZAG-treated; NL, normal.

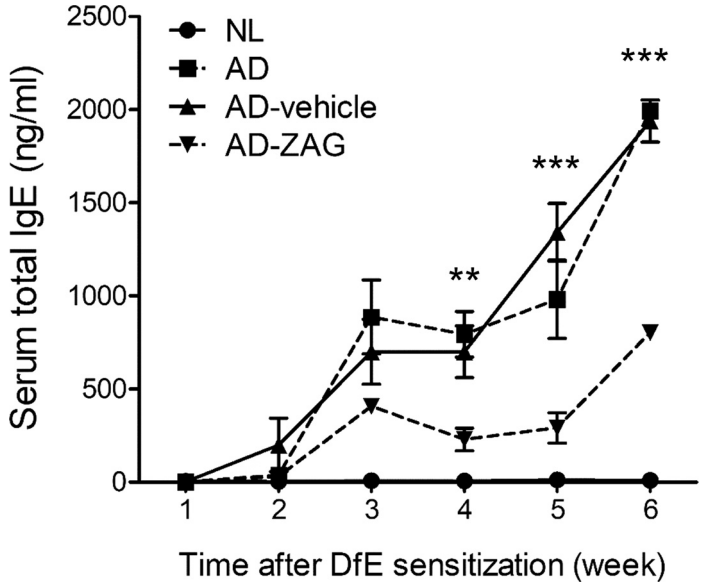

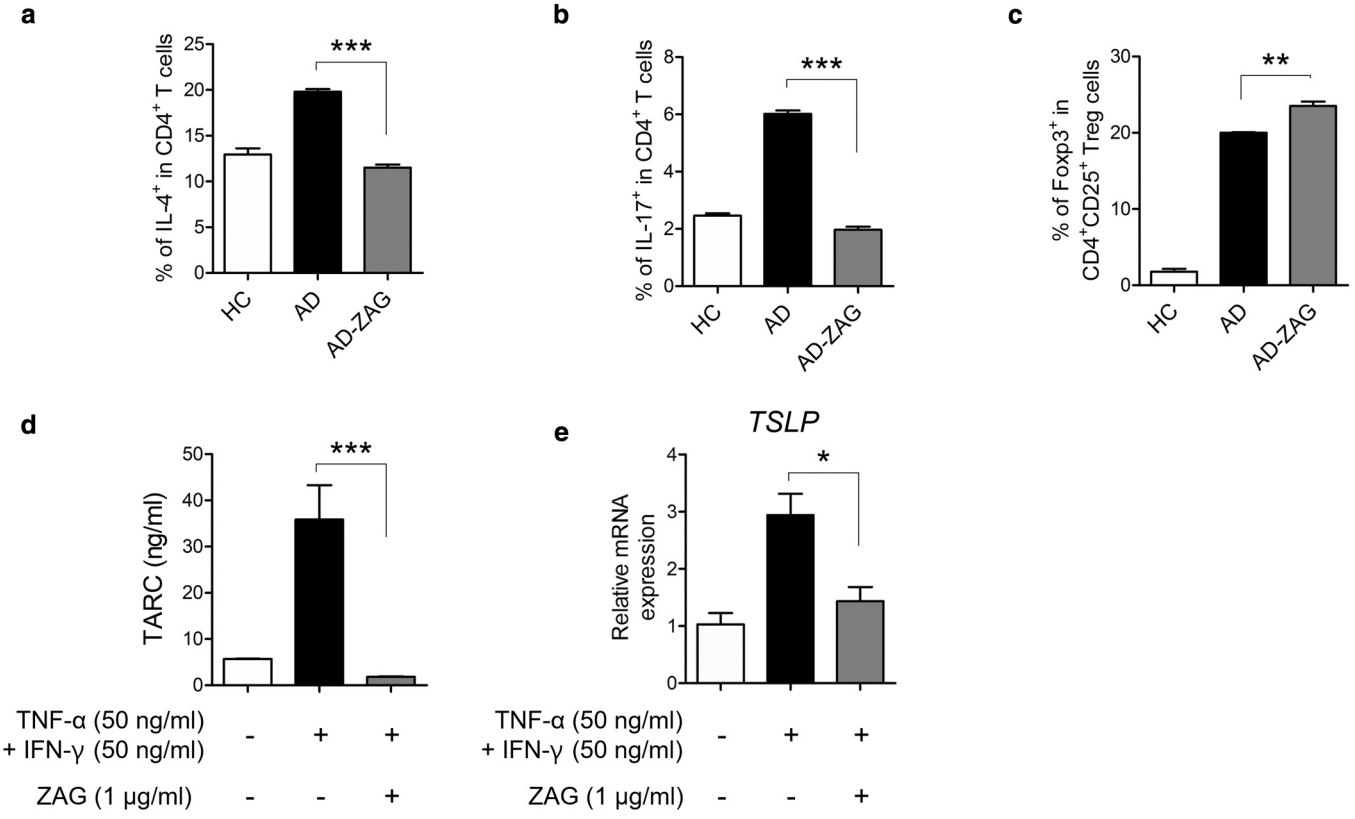

Supplementary Figure S5. Effects of ZAG in human T cells and normal human epidermal keratinocytes. Populations of IL-4$^+$ (**a**), IL-17$^+$ (**b**) cells in CD4$^+$ T cells, and Foxp3$^+$ cells in CD4$^+$CD25$^+$ Treg cells (**c**) were determined by FACS analysis in peripheral blood mononuclear cells from HC (n = 10), AD (n = 16), and AD (n = 16) treated with ZAG (2 μg/ml, 24 hours; $^{**}P < 0.01$, $^{***}P < 0.001$). Protein levels of (**d**) TARC and mRNA expression of (**e**) *TSLP* in normal human epidermal keratinocytes that were stimulated using TNF-α and IFN-γ (50 ng/ml each for 24 hours), and then with or without ZAG (1 μg/ml, 24 hours; $^{***}P < 0.001$, $^{*}P < 0.05$). AD, atopic dermatitis; HC, healthy control; TARC, thymus and activation-regulated cytokine; Treg, regulatory T cell.

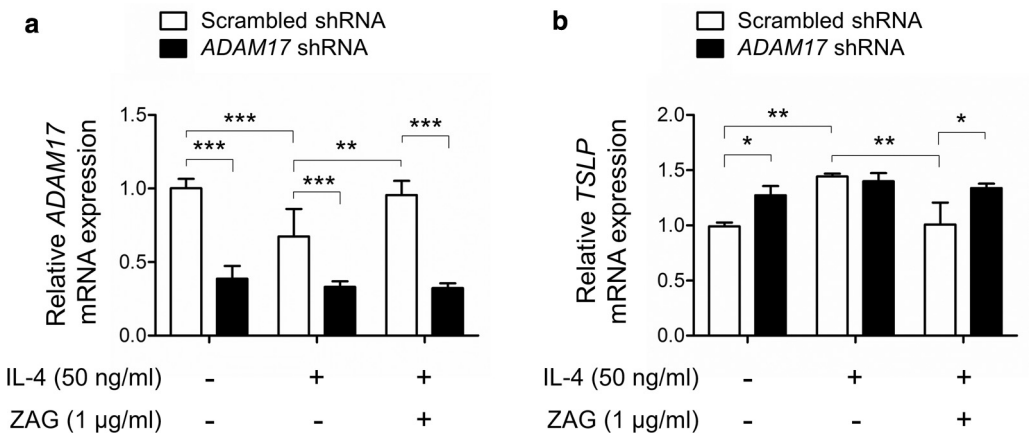

Supplementary Figure S6. ZAG regulates TSLP expression by ADAM17 in normal human epidermal keratinocytes. Quantitative real-time PCR analysis of (**a**) *ADAM17* and (**b**) *TSLP* mRNA expressions in scrambled and *ADAM17* shRNA-transfected normal human epidermal keratinocytes with the combined treatment of IL-4 and ZAG (*$P < 0.05$ ** $P < 0.01$, ***$P < 0.001$). sh, short hairpin RNA.

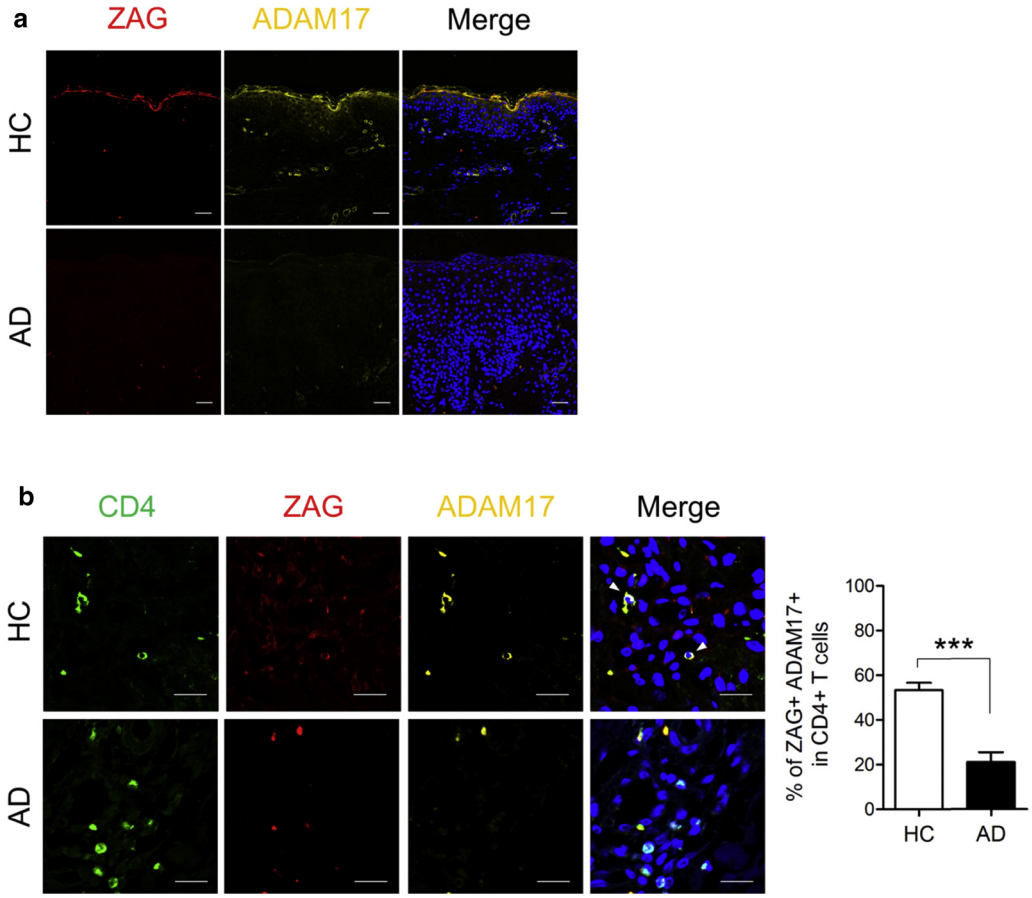

Supplementary Figure S7. Expressions of ZAG and ADAM17 in human HC and AD skin. (**a**) Immunofluorescence staining of ZAG (red) and ADAM17 (yellow) in the skin of HC (n = 9) and AD skin (n = 20). Scale bar = 20 μm. (**b**) Immunofluorescence staining of CD4 (green) and ZAG (red) in the dermis of HC and AD skin and the percentage of $ZAG^{+}ADAM17^{+}$ cells in $CD4^{+}$ T cells (***$P < 0.001$). Scale bar = 20 μm. AD, atopic dermatitis; HC, healthy control.

Supplementary Table S1. Baseline clinical characteristics of human samples

Characteristic	Healthy control	Atopic dermatitis
Sera for 2D-DIGE		
Patients (male/female), n	15 (9/6)	40 (20/20)
Age (y), mean ± SD	26.28 ± 0.79	27.83 ± 7.49
Total IgE (kU/l), mean ± SD	—	2,394.64 ± 2,128.26
EASI score, mean ± SD	—	24.90 ± 12.87
Sera for ELISA		
Patients, (male/female), n	36 (15/21)	90 (43/47)
Age (y), mean ± SD	29.38 ± 2.10	26.12 ± 6.36
Total IgE (kU/l), mean ± SD	—	1,762.85 ± 1,883.27
EASI score	—	19.24 ± 12.75
Skin for microarray		
Patients, (male/female), n	6 (4/2)	6 (3/3)
Age (y), mean ± SD	39.5 ± 17.33	33.33 ± 9.11
Total IgE (kU/l), mean ± SD	—	3,460.43 ± 1,712.65
EASI score	—	33.31 ± 20.28
Skin for immunohistochemistry and immunofluorescence staining		
Patients, (male/female), n	9 (6/3)	20 (10/10)
Age (y), mean ± SD	25.78 ± 7.63	28.65 ± 7.67
Total IgE (kU/l), mean ± SD	—	1,961.00 ± 2,086.91
EASI score, mean ± SD	—	18.67 ± 9.36
PBMCs for T-cell analysis		
Patients, (male/female), n	10 (6/4)	16 (7/9)
Age (y), mean ± SD	29.33 ± 1.27	20.38 ± 6.89
Total IgE (kU/l), mean ± SD	—	1,000.14 ± 1,443.61
EASI score	—	19.44 ± 13.81

Abbreviations: 2D-DIGE, 2-dimensional difference gel electrophoresis; EASI, Eczema Area and Severity Index; PBMC, peripheral blood mononuclear cell; SD, standard deviation.

Supplementary Table S2. Primer list

Gene symbol	Gene name	Assay ID
Human		
AZGP1	Zinc-alpha-2 glycoprotein	Hs00426651_m1
FLG	Filaggrin	Hs00856927_g1
CD36	Cluster of differentiation 36	Hs00354519_m1
FAS	Fas cell surface death receptor	Hs00236330_m1
PPARG	Peroxisome Proliferator activated receptor gamma	Hs01115513_m1
SLC27A4	Solute carrier family 27 member 4	Hs00192700_m1
CPT1A	Carnitine palmitoyltransferase I	Hs00912671_m1
ADIPOQ	Adiponectin	Hs00605917_m1
FASN	Fatty acid synthase	Hs01005622_m1
TSLP	Thymic stromal lymphopoietin	Hs00263639_m1
NOTCH1	Notch homolog 1	Hs01062014_m1
ADAM17	A disintegrin and a metallopeptidase 17	Hs01041915_m1
GAPDH	Glyceraldehyde 3-phosphate dehydrogenase	Hs02786624_g1
Mouse		
Flg	Filaggrin	Mm01716522_m1
Il-4	Interleukin 4	Mm00445259_m1
Il-17a	Interleukin 17a	Mm00439618_m1
Ifng	Interferon gamma	Mm01168134_m1
Foxp3	Forkhead box P3	Mm00475162_m1
Tslp	Thymic stromal lymphopoietin	Mm01157588_m1
Gapdh	Glyceraldehyde 3-phosphate dehydrogenase	Mm99999915_g1